Talanta 195 (2019) 401–406

Contents lists available at ScienceDirect

Talanta

journal homepage: www.elsevier.com/locate/talanta

Label-free identification of trace microcystin-LR with surface-enhanced Raman scattering spectra

Shixuan He[a,b,*], Wanyi Xie[a], Shaoxi Fang[a], Daming Zhou[a], Khouloud Djebbi[a], Zhiyou Zhang[b], Jinglei Du[b], Chunlei Du[a,b,*], Deqiang Wang[a,**]

[a] Chongqing Key Laboratory of Multi-scale Manufacturing Technology, Chongqing Institute of Green and Intelligent Technology, Chinese Academy of Sciences, 266 Fangzheng Ave, ShuiTu Technology Development Zone, Beibei District, Chongqing 400714, PR China
[b] Physics Department, Sichuan University, 29 Wangjiang Road, Chengdu, Sichuan 610064, PR China

ARTICLE INFO

Keywords:
Microcystin-LR
Surface-enhanced Raman scattering
Principal component analysis

ABSTRACT

The analysis of trace microcystin-LR (MC-LR) plays important roles in environmental fields, especially in monitoring domestic water quality and safety, since it has particularly harmful effect on wild and domestic animals as well as humans at low doses. Herein, we combine confocal Raman spectroscopy with SERS-AG substrate to characterize the "fingerprint" information of MC-LR directly. High sensitivity of SERS-AG substrates was verified by utilizing the probe molecule Rhodamine 6 G. Mapping spectra demonstrated good reproducibility of MC-LR identification with label-free surface-enhanced Raman scattering (SERS) strategy. Differences between SERS spectra of MC-LR and R6G, microcystin-RR were evaluated by calculating their scores and loading weights with an unsupervised exploratory principal component analysis method. Then, relationship between Raman intensities and concentrations was preliminary analyzed with SERS spectra of MC-LR and the lowest concentration of MC-LR identification was 10^{-6} mg L^{-1} while using SERS-AG substrate. Thereafter, 68.6% quantitative recovery of 10^{-3} mg L^{-1} MC-LR in tap water samples was obtained by the proposed label-free SERS method. These results showed that confocal Raman spectroscopy with label-free surface-enhanced Raman scattering strategy can handle the identification of trace MC-LR for monitoring water quality and safety worldwide in future.

1. Introduction

Nowadays, human activities exacerbated water blooms frequently in reservoirs, lakes and gulfs [1,2]. When algal apoptosis in water blooms, the most common toxins microcystins (MCs), which were released from cyanobacteria, have particularly harmful effect on wild and domestic animals as well as humans at low doses [3]. Specifically, MCs, a class of cyclic heptapeptide cyanotoxins with more than 80 structurally similar forms, can cause liver and kidney damage by inhibiting protein phosphatases 1 and 2 A activity [4,5]. Among them, microcystin-LR (MC-LR) is the most frequently encountered toxin in the family of MCs. And, World Health Organization provides a provisional guideline value of 1 μg L^{-1} as maximum allowable MC-LR concentration in drinking water [6]. Therefore, trace MC-LR identification plays important roles in environmental safety and human health fields. However, it is challenging to establish a sensitive, non-destructive, time saving, and label-free method for MC-LR identification so as to monitor water quality and safety worldwide.

Currently, a variety of molecular biology methods have been used for sensitive MC-LR detection, such as electrochemical biosensors [7], high performance liquid chromatography (HPLC) [8,9], and immunoassay [10,11]. Nevertheless, quite complicated procedures such as iterative polishing for electrodes surface modification limit the application of electrochemical biosensors. Moreover, HPLC technique is time-consuming and lacks of sensitivity without separation and preconcentration. In addition, immunoassay strongly depends on the stability of antibody and suffers from multi-step operations too. Therefore, a rapid and sensitive analytical method is urgent for identification and

Abbreviations: MCs, microcystins; MC-LR, microcystin-LR; MC-RR, microcystin-RR; HPLC, high performance liquid chromatography; DCDR, drop coating deposition Raman; SERS, Surface-Enhanced Raman Scattering; PCA, principal component analysis; RSD, Relative Standard Deviation; ND, not detected

* Corresponding authors at: Chongqing Key Laboratory of Multi-scale Manufacturing Technology, Chongqing Institute of Green and Intelligent Technology, Chinese Academy of Sciences, 266 Fangzheng Ave, ShuiTu Technology Development Zone, Beibei District, Chongqing 400714, PR China.
** Corresponding author.
E-mail addresses: heshixuan@cigit.ac.cn (S. He), cldu@cigit.ac.cn (C. Du), dqwang@cigit.ac.cn (D. Wang).

https://doi.org/10.1016/j.talanta.2018.11.072
Received 27 September 2018; Received in revised form 8 November 2018; Accepted 22 November 2018
Available online 23 November 2018
0039-9140/

quantitative analysis of trace MC-LR in drinking water.

Raman spectroscopy provides unique "fingerprint" information that reflects vibration or rotation of molecular bond, configuration and conformation of polar molecule. It is an effective method for molecular identification, even the discrimination of subtle differences among molecular isomers [12,13]. Combined with solid-phase extraction (SPE) technique, drop coating deposition Raman (DCDR) method is proposed for variant identification of seven MCs and quantitation of MC-LR as low as 1 $\mu g\,L^{-1}$. But, extraction processes for SPE and smaller Raman scattering cross sections for DCDR greatly restrict the rapid detection of trace MC-LR in water bodies [14,15]. Thereafter, aptamers driven Au nanoflowers-Ag nanoparticles core-satellite assemblies achieve sensitive detection of MC-LR as low as 0.01 nM with labeled Surface-Enhanced Raman Scattering (SERS) technology [16]. Moreover, gold coated magnetic nanoparticles (nanopillar), functionalized with MC-LR antibody, are used to selective capture the trace MC-LR in complex water bodies. MC-LR quantification already lowers to the clinically required limit of detection with nanopillar [17]. However, much background information from synthetic or modified substrates has hindered the characteristic "fingerprint" spectral analysis of trace MC-LR. In addition, trace MC-LR has not been directly identified by using SERS technology with their real Raman characteristic information.

Herein, we use confocal Raman spectroscopy to focus the incident laser beam on SERS-AG substrate to obtain enhanced Raman characteristic information of trace MC-LR. Firstly, the sensitivity and reproducibility of SERS-AG substrates are verified by probe molecule Rhodamine 6 G (R6G) and MC-LR respectively. Then, Raman characteristic information of MC-LR, which are resolved with SERS mapping spectra, are discussed with its isomer microcystin-RR (MC-RR) and disturbed dye molecules R6G by an unsupervised exploratory principal component analysis (PCA) [18]. Thereafter, trace MC-LR in ultrapure and tap water samples are analyzed with their SERS spectra respectively. This approach could provide an efficient SERS technology for MC-LR identification and then monitoring the water quality and safety in future.

2. Experimental section

2.1. Sample preparation

The probe molecule R6G (Sigma, 99%), L-leucine (Adamas, 99%) and L-arginine (Adamas, 99%) were obtained from Titan (Shanghai, China). Then, 10^{-6} M, 10^{-7} M, 10^{-8} M, 10^{-9} M, and 10^{-10} M R6G solution were prepared with ultrapure water. MC-LR, MC-RR standards (PriboFast, 95%) were purchased from Pribolab (Qingdao, China). The solid MC-LR, MC-RR were dissolved to the concentration of 100 $mg\,L^{-1}$ in ultrapure water as stock suspension and then stored at − 20 °C. Thereafter, 10 $mg\,L^{-1}$ MC-RR and 10^{-6} $mg\,L^{-1}$ − 10 $mg\,L^{-1}$ MC-LR solution were prepared with ultrapure water for spectral measurements. And, SERS spectra of 10^{-3} $mg\,L^{-1}$ − 10^{-1} $mg\,L^{-1}$ MC-LR solution, prepared with untreated or filtered tap water by using 0.22 μm filter, were obtained to verify the effectiveness of MC-LR determination in tap water by using SERS technology. In addition, the SERS substrates - SERS-AG were obtained from Ocean Optics (Shanghai, China).

2.2. Raman spectroscopy and measurements

A Renishaw (Wotton-under-Edge, Gloucestershire, UK) inVia micro-Raman spectroscopy system, equipped with a Peltier cooled CCD detector (−70 °C) and a 532 nm DPSS laser (maximum laser power: 50 mw), was used to collect back-scattered Raman signals upon 2400 lines mm^{-1} grating. Prior to Raman measurements, the spectrometer was calibrated with Raman shift of silicon at 520 cm^{-1} every day. The spectral range was from 596 cm^{-1} to 1760 cm^{-1} and the integration time for each spectrum was 10 s.

Normally, 2 μL MC-LR and MC-RR aqueous (10 $mg\,L^{-1}$) were dried on Al substrates respectively. Then, DCDR spectra of MC-LR and MC-RR were collected by using a Leica microscope with 100 × objective (NA: 0.85; spot size: 0.8 μm). Laser power on samples was about 10 mW. And, the number of acquisition was 10 times for each measurement. While for SERS measurements, 30 μL samples were deposited on the SERS-AG substrates. A Leica microscope with 50 × (NA: 0.75; Spot size: 1 μm) and 20 × (NA: 0.4; Spot size: 1.6 μm) objectives was used to focus incident laser on the R6G and MC-LR, MC-RR molecules respectively. Thereafter, 1% (0.2 mW) and 10% (2 mW) of laser powers were used to excite Raman scattering signals of R6G and MC-LR, MC-RR with 1 acquisition time respectively.

2.3. Principal component analysis (PCA)

An unsupervised exploratory principal component analysis (PCA) was used to assess the impacts of interferences - R6G and MC-RR on the SERS detection of MC-LR. Each 20 SERS spectra of R6G (10^{-6} M), MC-RR (10 $mg\,L^{-1}$), MC-LR (10 $mg\,L^{-1}$) were modeled to obtain their PCA scores and loading weights. Differences of Raman characteristic information among R6G, MC-RR and MC-LR can be visualized by PC scores and loading weights plots.

3. Results and discussion

Firstly, absorption spectra of 10^{-1} $mg\,L^{-1}$, 1 $mg\,L^{-1}$, 5 $mg\,L^{-1}$, and 10 $mg\,L^{-1}$ MC-LR samples were detected by using a UV spectrometer (PERSEE TU-1950, Beijing, China). As shown in Fig. S1, characteristic absorption peak of MC-LR - wavenumber at 239 nm [19] showed a liner relationship with their corresponding concentrations. And, little peak can be found in the absorption spectra of 10^{-1} $mg\,L^{-1}$ MC-LR. That is to say, with no other pretreatments, we can't reach the limit of detection for MC-LR - maximum allowable level in drinking water by using UV spectrometer. Therefore, based on localized surface plasma enhanced strategy, surface-enhanced Raman scattering spectra have been trying to identify the trace MC-LR toxin in tap water environment.

3.1. SERS enhanced performances verification

SERS-AG, used as SERS substrate, was fabricated by coating AgNPs on filter. We can observe the structure of SERS-AG substrate with SEM (JSM-7800F JEOL, Japan) in detail. As shown in Fig. S2, many nanogaps between adjacent AgNPs on filter membrane can greatly enhance the Raman scattering intensity with localized surface plasmas. Firstly, in order to quantitative analysis of trace MC-LR with surface-enhanced Raman scattering spectra, probe molecule R6G was used to verify the SERS enhanced performance of SERS-AG substrate. As shown in Fig. 1, much characteristic "fingerprint" information of R6G molecules was

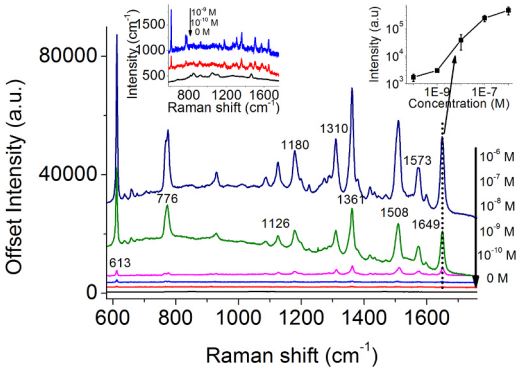

Fig. 1. SERS spectra for different concentrations of R6G with SERS-AG substrates. The left inset shows the enlarged SERS spectra for 10^{-9} M, 10^{-10} M R6G and substrate. The right inset shows the relationship between Raman intensities at 1649 cm^{-1} and their corresponding concentrations of R6G on double logarithmic coordinate system.

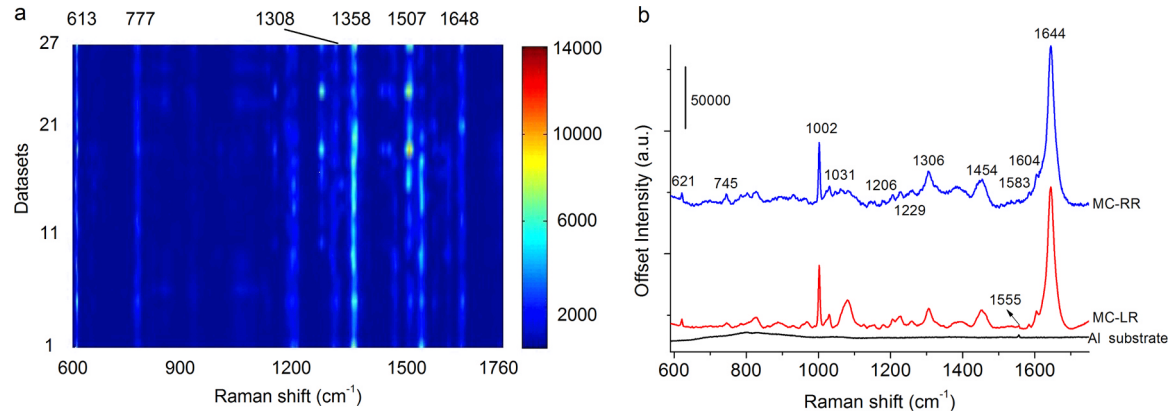

Fig. 2. (a) SERS mapping spectra of 10 mg L^{-1} MC-LR on SERS-AG substrate. (b) DCDR spectra of 10 mg L^{-1} MC-LR and MC-RR on the Al substrates.

obtained with SERS technology by using SERS-AG substrates, such as 613 cm^{-1}, 776 cm^{-1}, 1126 cm^{-1}, 1180 cm^{-1}, 1310 cm^{-1}, 1361 cm^{-1}, 1508 cm^{-1}, 1573 cm^{-1}, and 1649 cm^{-1}. For 10^{-6} M – 10^{-10} M R6G samples, Raman characteristic information demonstrated a decreasing tendency in comparison with concentrations of R6G, as shown in the right inset of Fig. 1. Especially, the left inset of Fig. 1 shows that primary "fingerprint" peaks can be measured on the SERS spectra of 10^{-10} M R6G sample. In all, the limit of detection would be lower than 10^{-10} M for probe molecule R6G by using SERS-AG substrate. Thereafter, trace MC-LR could be directly identified with SERS spectra by using SERS-AG.

3.2. Identification of MC-LR with SERS spectra and its band assignments

Herein, DCDR and SERS spectra were obtained with Al and SERS-AG substrates respectively, as shown in Fig. 2 and Fig. S3. Much characteristic Raman "fingerprint" information of MC-LR was clearly appeared on background of substrates, such as primary characteristic Raman shifts 521 cm^{-1}, 745 cm^{-1}, 1002 cm^{-1}, 1031 cm^{-1}, 1206 cm^{-1}, 1229 cm^{-1}, 1306 cm^{-1}, 1454 cm^{-1}, 1583 cm^{-1}, 1644 cm^{-1} on DCDR spectra and 613 cm^{-1}, 777 cm^{-1}, 1000 cm^{-1}, 1127 cm^{-1}, 1186 cm^{-1}, 1193 cm^{-1}, 1271 cm^{-1}, 1308 cm^{-1}, 1358 cm^{-1}, 1380 cm^{-1}, 1434 cm^{-1}, 1507 cm^{-1}, 1540 cm^{-1}, 1575 cm^{-1}, 1613 cm^{-1}, 1648 cm^{-1} on SERS spectra of MC-LR.The characteristic Raman shifts and band assignments for Raman spectra of MC-LR were detailed in Table 1.

Based on structure of MCs (Fig. S4), we knew that L-leucine (Leu) and L-arginine (Arg) were specificity amino acids groups which were distinguished MC-LR from other isomers. Especially, there was only a difference at X position between MC-RR and MC-LR, Arg for MC-RR and Leu for MC-LR, as shown in Fig. S4. Therefore, normal Raman spectra of solid Arg and Leu were measured to verify the SERS spectral band assignments of MC-LR molecule. As shown in Fig. S5b, some characteristic Raman shifts of Leu, such as 770 cm^{-1}, 999 cm^{-1}, 1128 cm^{-1}, 1186 cm^{-1}, 1313 cm^{-1}, 1360 cm^{-1}, 1374 cm^{-1}, and 1580 cm^{-1}, were similar to characteristic "fingerprint" information of MC-LR. These bands, only a few shifts from SERS spectra of MC-LR, can be assigned as C-C stretching, NH_3^+ deformation and rocking, C_α-H bending, CH_2 scissoring and COO^- stretching vibrations of Leu respectively. Moreover, some characteristic Raman information of MC-LR – 1308 cm^{-1} and 1434 cm^{-1} can be assigned as C_β-C_α-H, C_α-H bending, N-H rocking, C=O stretching, C_β twisting and C_γ rocking vibrations of Arg (Fig. S5a).

In addition, there were some shifts between SERS and DCDR spectra of MC-LR in previous work [14]. These shifts may be due to the interaction between MC-LR molecules with metal nanoparticles. Meanwhile, much Raman characteristic information of MC-LR was excited over background signal, owing to localized surface plasma enhanced of SERS-AG substrate. Moreover, some Raman shifts, which came from enhanced mechanism between different SERS substrates and molecules, were also existed in SERS-AG in comparison with paper-based SERS substrates coating with gold nanoparticles (Gold nanopillar) [17]. Thereafter, we have investigated the reproducibility of SERS-AG substrate by using Raman mapping spectra of 10 mg L^{-1} MC-LR (Fig. 2). The primary characteristic Raman shifts of MC-LR were clearly shown in the mapping spectra, such as 613 cm^{-1}, 777 cm^{-1}, 1308 cm^{-1}, 1358 cm^{-1}, 1507 cm^{-1}, and 1648 cm^{-1}. The results indicated that SERS spectra of MC-LR were better reproducible by using the SERS-AG substrate.

3.3. Impact of interferences on SERS Identification of MC-LR

The influences of other water pollution - isomer MC-RR and disturbed dye molecules R6G on the identification of MC-LR have been investigated with proposed SERS technology. No obviously Raman characteristic differences were shown in DCDR spectra of MC-LR and MC-RR (Fig. 2b), SERS spectra of MC-LR, MC-RR and R6G (Fig. S6), except only little shifts or intensity differences. Therefore, MC-LR identification would be disturbed with R6G and MC-RR by using the proposed SERS strategy, only considering the characteristic Raman shifts. Thereafter, the detailed differences were mined with SERS spectra of MC-LR, MC-RR, and R6G by an unsupervised exploratory PCA analysis method. As shown in Fig. 3a, SERS spectra of MC-LR were completely separated from that of R6G and MC-RR with PCA scores on PC1, PC2, and PC3, retained 99.75% of total variances. At the same time, the corresponding loading weights Lw1, Lw2 and Lw3 also showed some characteristic Raman "fingerprint" information, such as 613 cm^{-1}, 775 cm^{-1}, 1145 cm^{-1}, 1270 cm^{-1}, 1358 cm^{-1}, 1507 cm^{-1}, 1540 cm^{-1}, 1652 cm^{-1}, which was used to discriminate MC-LR from interferences. In all, "fingerprint" characteristics - both Raman shifts and intensities were effective for molecular discrimination with Raman spectroscopy.

3.4. Label-free identification of trace MC-LR with SERS spectra

Thereafter, different concentrations of MC-LR samples were measured with confocal Raman spectroscopy by using SERS-AG substrates. The average Raw and corrected SERS spectra of 10^{-6} mg L^{-1} – 10 mg L^{-1} MC-LR samples are shown in Fig. S7 and Fig. 4a respectively. While processing with baseline correction method [20], Raman characteristic information of MC-LR was obviously obtained in comparison with background of SERS-AG substrate. Fig. 4a also demonstrated that Raman intensities decreased gradually when concentrations of MC-LR reduced. Meanwhile, background signals dominated gradually while concentrations of MC-LR decreased. We can infer that some Raman characteristic information of MC-LR would be covered by background signals as long as its concentration decreased further. In

Table 1
Band assignments for Raman spectra of MC-LR.

Raman shift (cm^{-1})			Band assignments [15]
SERS-AG	DCDR	Gold nanopillar [17]	
613	621	643	C-H in-plane bending, C-C twisting, deformation of phenyl ring; COO^- wagging of[a]Glu and[b]Me-Asp.
777	745	753	C-H out-of-plane bending of phenyl ring; COO^- bending, CH_2 rocking of Glu.
1000	1002	1019	In-plane bending, symmetric breathing, C-C symmetric stretching of phenyl ring; C-C and C-O stretching of Glu; C-C stretching of[c]Leu.
1127	–	1124	NH_3^+ deformation of Glu and Leu residues.
1186	–	1181	NH_3^+ rocking of Leu residue.
1204	1206	1211	CH_2 twisting and rocking of Glu residue.
1271	1229	1239, 1261	Amide III vibration.
1308	1306	1305	H-C_α-$C_{terminal}$ vibrations of[d]Ala; C_β-C_α-H vibrations of Ala and[e]Arg; CH_2 twisting, rocking, and deformation of Ala and Glu; CH_2 wagging of Glu; C_α-H bending of Glu, Arg, and Leu; N-H rocking, C=O stretching, C_β twisting and C_γ rocking of Arg; C-H bending and CH_2 wagging of[f]Adda; C-H in-plane bending and stretching of phenyl ring.
1358, 1380	1386	1367	COO^- stretching, CO stretching, CH_3 symmetric bending and CH_2 scissoring of Ala, Leu and Glu residues.
1507	–	1493	Symmetric NH_3^+ bending of Ala residue.
1540	1555	1536	Amide II vibration.
1575	1583	1582	Phenyl ring; COO^- stretching of Adda and Leu residues.
1648	1644	–	Amide I, water in aqueous peptide sample.

[a] Glu: D-glutamic.
[b] Me-Asp: N-methyl-D-aspartic acid.
[c] Leu: L-leucine.
[d] Ala: D-alanine.
[e] Arg: L-arginine.
[f] Adda: 3-amino-9-methoxy-2,6,8-trimethyl-10-phenyl-4,6-decadienoic acid.

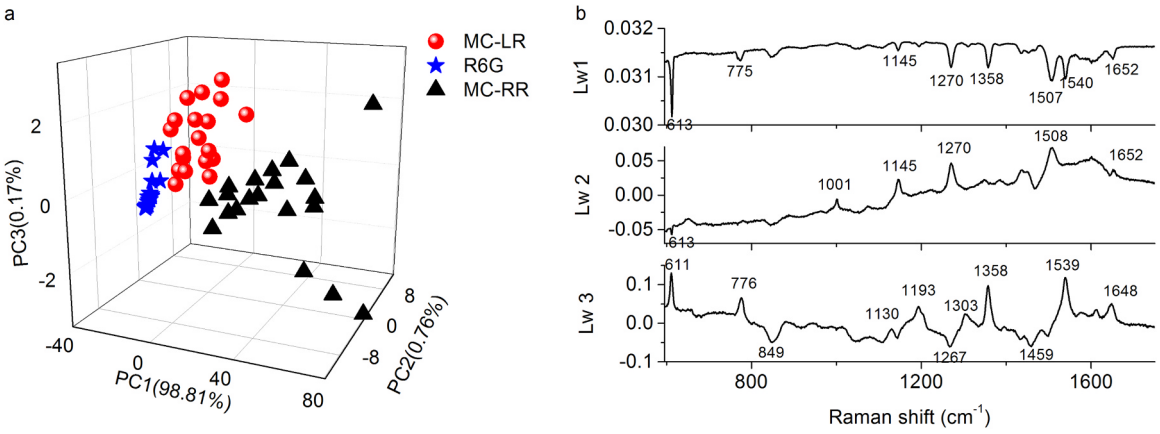

Fig. 3. Impacts of R6G and MC-RR interferences on SERS identification of MC-LR. (a) PCA scores and (b) loading weights plot for SERS spectra of MC-LR, MC-RR, and R6G.

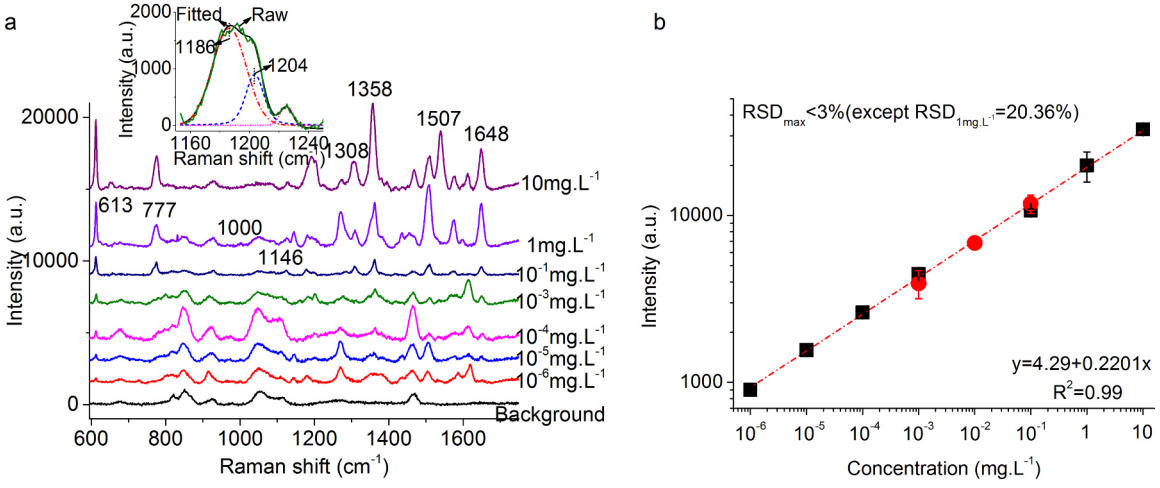

Fig. 4. (a) SERS spectra for different concentrations of MC-LR with SERS-AG substrates after baseline correction (the inset shows the fitted result with Lorentz functions) and (b) Liner relationship between Raman intensities at 613 cm^{-1} and concentrations of MC-LR on double logarithmic coordinate system (Black Square-ultrapure water; Red Circle - tap water).

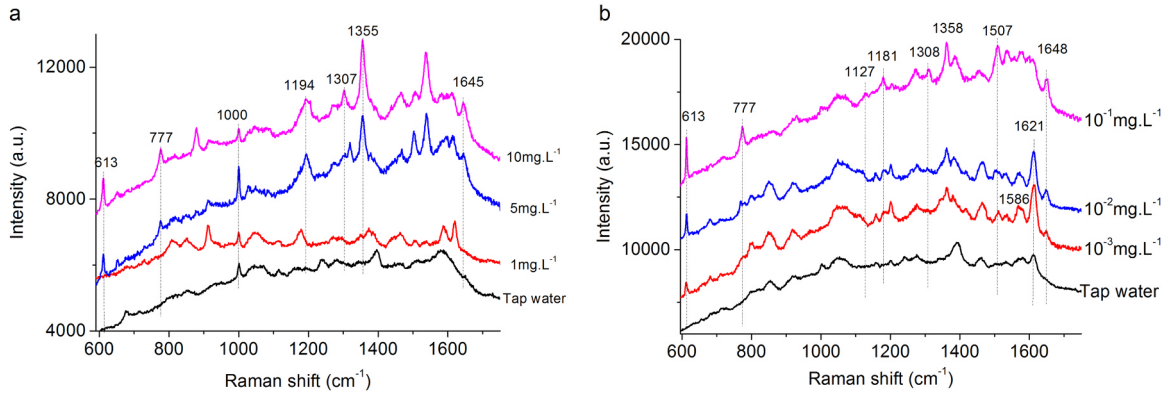

Fig. 5. SERS spectra for different concentrations of MC-LR with SERS-AG substrates in tap water samples. (a) un-filtered water samples; (b) filtered water samples.

Table 2
Detection of MC-LR in tap water samples by using the proposed method (n = 3).

Tap water	Concentration (mg L^{-1})			Recovery (%)
	Background	Spiked	Found	
1	[a]ND	10^{-1}	1.01×10^{-1}	101.0
2	ND	10^{-2}	8.62×10^{-3}	86.2
3	ND	10^{-3}	6.86×10^{-4}	68.6

[a] ND: not detected.

addition, CH_2 twisting and rocking vibrations of D-glutamic acid residue (1204 cm^{-1}) can be separated from NH_3^+ rocking of L-leucine residue (1186 cm^{-1}) by fitting with *Lorentz* functions, as shown in Fig. 4a (inset).

Then, C-H in-plane bending, C-C twisting, deformation vibrations of phenyl ring and COO^- wagging vibration of Glu/Me-Asp − 613 cm^{-1} was fitted to analyze the relationship between Raman intensities and concentrations of MC-LR. It was demonstrated with linear fitting of Raman intensities at the interval from 10^{-6} mg L^{-1} to 10 mg L^{-1} on the double logarithmic coordinate system (Fig. 4b). The adjusted coefficient of determination achieved 0.99 (RSD < 3%, except for 1 mg L^{-1} MC-LR), while the higher error appeared for the concentration of 1 mg L^{-1}. Currently, the lowest concentration of MC-LR identification by using SERS-AG substrate was 10^{-6} mg L^{-1} - lower than provisional guideline value for MC-LR in drinking water throughout the world.

At last, SERS spectra of simulated water samples - tap water spiked with different concentrations of MC-LR were measured to verify the effectiveness of SERS-AG substrates in environmentally realistic conditions. As shown in Fig. 5a, Raman characteristic information of MC-LR was hidden by background signals, even if 1 mg L^{-1} MC-LR was spiked in the untreated tap water sample. While MC-LR was spiked in filtered tap water samples, much Raman characteristic information was both obtained in the SERS spectra of tap water samples spiked with 10^{-3} mg L^{-1}, 10^{-2} mg L^{-1}, and 10^{-1} mg L^{-1} MC-LR (Fig. 5b). And, at least 68.6% quantitative recovery for 10^{-3} mg L^{-1} MC-LR - provisional guideline value for MC-LR in drinking water, was obtained with SERS spectra of filtering (0.22 μm) treated water samples (Table 2). At the same time, Raman spectra of untreated and filtered tap water samples showed similar spectral information which came from fluorescence or "fingerprint" characteristic of impurities in the realistic water samples and SERS-AG substrates themselves. In addition, SERS of MC-LR in tap water sample showed much interference peaks than that of tap water sample, such as 1586 cm^{-1} and 1621 cm^{-1} in Fig. 5b. These result demonstrated that characteristic "fingerprint" information of MC-LR was enhanced by SERS-AG substrates along with SERS enhancing of interferences in realistic water samples and SERS-AG substrates themselves. Above all, SERS identification of trace MC-LR was affected by impurities in the realistic water samples. Therefore, pretreatment and separation technologies would be very necessary for trace MC-LR identification in environmentally conditions.

4. Conclusions

Trace microcystin-LR has been identified by label-free using surface-enhanced Raman scattering strategy. The sensitivity of SERS-AG substrates was verified with probe molecule R6G firstly. Raman characteristic information of MC-LR were obtained by using SERS-AG substrates. And, better reproducibility was demonstrated with mapping spectra of MC-LR. Then, little differences between SERS spectra of MC-LR and R6G were evaluated with scores and loading weights by an unsupervised exploratory principal component analysis. Thereafter, relationship between Raman intensities and concentrations was preliminary analysis with SERS spectra of MC-LR and a level of 10^{-6} mg L^{-1} MC-LR was obtained. In addition, effectiveness of SERS-AG substrates in environmentally realistic conditions have been verified with simulated water samples. The result demonstrated that surface enhanced performance of SERS substrate would be improved to handle the label-free identification of trace MC-LR for monitoring water quality and safety problem worldwide.

Acknowledgements

This work was supported by research funding from Natural Science Foundation of Chongqing, China (Grant No. cstc2018jcyjAX0310), Chongqing Science and Technology Innovation in Social Livelihood of the People (Grant Nos. cstc2015shmszxX0002), National Natural Science Foundation of China (Grant No. 21507131, 41603089).

Declarations of interest

None.

Appendix A. Supporting information

Supplementary data associated with this article can be found in the online version at doi:10.1016/j.talanta.2018.11.072.

References

[1] W.J. Cai, X. Hu, W.J. Huang, M.C. Murrell, J.C. Lehrter, S.E. Lohrenz, W. Chou, W. Zhai, J.T. Hollibaugh, Y. Wang, P. Zhao, X. Guo, K. Gundersen, M. Dai, G. Gong, Acidification of subsurface coastal waters enhanced by eutrophication, Nat. Geosci. 4 (11) (2011) 766–770.

[2] S. He, W. Xie, P. Zhang, S. Fang, Z. Li, P. Tang, X. Gao, J. Guo, C. Tlili, D. Wang, Preliminary identification of unicellular algal genus by using combined confocal resonance Raman spectroscopy with PCA and DPLS analysis, Spectrochim. Acta A

Mol. Biomol. Spectrosc. 190 (2018) 417–422.
[3] M. Gantar, R. Sekar, L.L. Richardson, Cyanotoxins from black band disease of corals and from other coral reef environments, Microb. Ecol. 58 (2009) 856–864.
[4] J.A. Meriluoto, L.E. Spoof, Cyanotoxins: sampling, sample processing and toxin uptake, Adv. Exp. Med. Biol. 619 (2008) 483–499.
[5] B. Zegura, A. Straser, M. Filipic, Genotoxicity and potential carcinogenicity of cyanobacterial toxins-a review, Mutat. Res. 727 (2011) 16–41.
[6] World Health Organization (WHO), Guidelines for Drinking Water Quality. Vol.1, Recommendations/World Health Organization, Second ed., World Health Organization, Geneva, Switzerland, 1998, p. 36.
[7] J. Zhang, Y. Sun, H. Dong, X. Zhang, W. Wang, Z. Chen, An electrochemical non-enzymatic immunosensor for ultrasensitive detection of microcystin-LR using carbon nanofibers as the matrix, Sens. Actuators B Chem. 233 (2016) 624–632.
[8] Y.C. Guo, A.K. Lee, R.S. Yates, S. Liang, P.A. Rochelle, Analysis of microcystins in drinking water by ELISA and LC/MS/MS, J. Am. Water Works Assoc. 109 (3) (2017) 13–25.
[9] W. Ni, J. Zhang, Y. Luo, Microcystin accumulation in bighead carp (Aristichthys nobilis) during a Microcystis-dominated bloom and risk assessment of the dietary intake in a fish pond in China, Environ. Sci. Pollut. Res. 24 (10) (2017) 8894–8902.
[10] M. Liu, J. Yu, X. Ding, G. Zhao, Photoelectrochemical aptasensor for the sensitive detection of microcystin-LR based on graphene functionalized vertically-aligned TiO_2 nanotubes, Electroanalysis 28 (1) (2016) 161–168.
[11] W. Zhang, C. Han, B. Jia, C. Saint, M. Nadagouda, P. Falaras, L. Labrini Sygellou, V. Vasileia Vogiaz1, D.D. Dionysiou, A 3D graphene-based biosensor as an early microcystin-LR screening tool in sources of drinking water supply, Electrochim. Acta 236 (2017) 319–327.
[12] K. Kneipp, H. Kneipp, I. Itzkan, R.R. Dasari, M.S. Feld, Ultrasensitive chemical analysis by Raman spectroscopy, Chem. Rev. 99 (1999) 2957–2976.
[13] A.K. Samal, L. Polavarapu, S. Rodal-Cedeira, L.M. Liz-Marzán, J. Pérez-Juste, I. Pastoriza-Santos, Size tunable Au@ Ag core-shell nanoparticles: synthesis and surface-enhanced Raman scattering properties, Langmuir 29 (2013) 15076–15082.
[14] R.A. Halvorson, P.J. Vikesland, Drop coating deposition Raman (DCDR) for microcystin-LR identification and quantitation, Environ. Sci. Technol. 45 (2011) 5644–5651.
[15] R.A. Halvorson, W. Leng, P.J. Vikesland, Differentiation of microcystin, nodularin, and their component amino acids by drop-coating deposition raman spectroscopy, Anal. Chem. 83 (2011) 9273–9280.
[16] Y. Zhao, X. Yang, H. Li, Y. Luo, R. Yu, L. Zhang, Y. Yang, Q. Song, Au nanoflower-Ag nanoparticle assembled SERS-active substrates for sensitive MC-LR detection, Chem. Commun. 51 (95) (2015) 16908–16911.
[17] W.A. Hassanain, E.L. Izake, M.S. Schmidt, G.A. Ayoko, Gold nanomaterials for the selective capturing and SERS diagnosis of toxins in aqueous and biological fluids, Biosens. Bioelectron. 91 (2017) 664–672.
[18] S. He, W. Xie, W. Zhang, L. Zhang, Y. Wang, X. Liu, Y. Liu, C. Du, Multivariate qualitative analysis of banned additives in food safety using surface enhanced Raman scattering spectroscopy, Spectrochim. Acta A Mol. Biomol. Spectrosc. 137 (2015) 1092–1099.
[19] Y. Shi, J. Wu, Y. Sun, Y. Zhang, Z. Wen, H. Dai, H. Wang, Z. Li, A graphene oxide based biosensor for microcystins detection by fluorescence resonance energy transfer, Biosens. Bioelectron. 38 (1) (2012) 31–36.
[20] S. He, W. Zhang, L. Liu, Y. Huang, J. He, W. Xie, P. Wu, C. Du, Baseline correction for Raman spectra using an improved asymmetric least squares method, Anal. Methods 6 (2014) 4402–4407.